ELSEVIER

Biophysical Chemistry 79 (1999) 205–217

Biophysical Chemistry

Effect of Na^+ concentration on the subgel phases of negatively charged phosphatidylglycerol

Michiko Kodama*, Hiroyuki Aoki, Takahiro Miyata

Department of Biochemistry, Faculty of Science, Okayama University of Science, 1-1 Ridai-cho, Okayama 700-0005, Japan

Received 15 February 1999; received in revised form 29 March 1999; accepted 31 March 1999

Abstract

The effect of Na^+ concentration on the subgel phase of dimyristoylphosphatidylglycerol (DMPG) was investigated by differential scanning calorimetry (DSC) and negative stain electron microscopy, and the results were compared with dipalmitoylphosphatidylglycerol (DPPG). The conversion mode of DMPG vesicle to the subgel phase by annealing at 5°C was grouped into two types depending on whether Na^+ concentration is above or below 200–250 mM. For $[Na^+] > 200–250$ mM, the subgel phase of a crystalline superstructure of bilayers wrapped in a cylinder was attained during a 24-h period of annealing and transformed directly to the liquid crystal phase on heating. For $[Na^+] < 200–250$ mM, two subgel phases which transform to the gel phase on heating were observed after annealing up to 24 h. Both subgel phases showed belt-like structures composed of loosely and closely stacked lamellae, respectively, and their fractions were found to depend on Na^+ concentration. With a further annealing up to 30 days, only the closely stacked subgel phase converted subsequently into the cylindrical superstructure of a more ordered phase. Similar two subgel phases were detected for DPPG at $[Na^+] \leq 100$ mM. The difference in the relative enthalpy between the gel and subgel phases was investigated from the van der Waals interaction energy between the hydrocarbon chains.

Keywords: Phosphatidylglycerol; Subgel phase; Van der Waals interaction energy; Differential scanning calorimetry; Electron microscopy

1. Introduction

Acidic phospholipids, thus, negatively charged at neutral pH, have attracted attention of many investigators from the viewpoint of their structural and functional role in biomembranes, because lateral packings and interactions of the lipids in a fundamental bilayer structure are greatly influenced by environmental conditions of cations and protons [1–6]. In this connection, we have previously reported that dimyristoylphosphatidylglycerol (DMPG) vesicles prepared with

*Corresponding author. Tel.: +81-252-3161; fax: +81-86255-7700.

0301-4622/99/$ - see front matter
PII: S0301-4622(99)00053-8

NaCl aqueous solutions at different concentrations up to 100 mM show a marked Na^+ concentration-dependence in their multiplicities and sizes [7]. Furthermore, it has been found [8] that by a prolonged incubation at 5°C in the gel phase temperature, DMPG vesicles as large as 1 μm in size at $[Na^+] = 1000$ mM convert to a cylindrical superstructure similar to that formed in the presence of Ca^{2+} and Mg^{2+}[9–14]. In the present study, DMPG vesicles of widely differing multiplicities and sizes at different Na^+ concentrations below 1000 mM were annealed into the subgel phase from the gel phase at 5°C over a 30-day period and the effect of Na^+-concentration on the subsequent subgel phase was investigated. Studies on the subgel phases of PGs have been performed with a variety of buffer solutions in the presence of salts by other workers [15–19]. However, when these past studies are compared, we note some inconsistencies. From this viewpoint, considering the influence of cations such as Na^+[15,16] and tris + [17,18] contained as a component of buffer, we did not think it appropriate to use buffer solutions for vesicle preparations in the present study.

2. Materials and methods

2.1. Materials and sample preparation

1,2-Dimyristoyl- and 1,2-dipalmitoyl-*sn*-glycero-3-[phospho-*rac*-(1-glycerol)] (DMPG and DPPG, sodium salts) were purchased from Sigma Co., and used without further purification as thin-layer chromatography of these lipids showed a single spot. Dispersions of vesicles composed of each of DMPG and DPPG at a lipid concentration of ~2 mM were prepared as follows [20]: lipid films (~3 mg) were first prepared by removing chloroform from lipid stock solutions on a rotary evaporator, and then under high vacuum (10^{-4} Pa) to achieve complete removal of traces of the solvent. The dried lipid films were then suspended in aqueous solutions of NaCl (~2 ml) at concentrations of 20, 50, 80, 100, 200, 250 and 500 mM, respectively, and gently vortexed at desired temperatures above the T_M transitions. All vesicle samples were annealed at 5°C in a calorimetric cell over a period of a few days, beyond which an accurately controlled water bath (Haake F3-c) was used for thermal annealing. Lipid concentrations of the samples after DSC were estimated by a modified Bartlett phosphate assay [21].

2.2. High sensitivity differential scanning calorimetry

All calorimetric experiments were performed with a Microcal MC 2 differential scanning calorimeter equipped with a PC microcomputer system for automatic data collection and analysis. The lipid concentrations in the calorimetric experiments were in the range 1–2 mM with a calorimetric cell volume of 1.2 ml. A heating scanning rate of 45°C/h was used.

2.3. Electron microscopy

Negative stain electron microscopic experiments were performed with a JEOL JEM-2000EX electron microscope operated at 200 kV. Particular attention was paid to sodium phosphotungstate solution (pH ~ 7) used as a stainer because Na cation derived from the stain has the same effect on PG as that derived from NaCl, as is shown by comparisons of Fig. 1a with Fig. 2D(a) and of Fig. 1b with Fig. 2B(b). From this viewpoint, as long as the Na^+ concentration is lower than 100 mM, the vesicle samples were prepared in the presence of the stainer. For example, for $[Na^+] = 20$ mM, the lipid film (~3 mg) was suspended in 2 ml of 1% (w/v) sodium phosphotungstate solution because the Na^+ concentration of the stainer solution is approximately 20 mM. For $[Na^+] = 100$ mM, a mixture of 1 ml of 2% sodium phosphotungstate solution ($[Na^+] = 40$ mM) and 1 ml of 160 mM NaCl solution was used. These vesicle samples likewise were annealed, and then checked by DSC prior to electron microscopic experiments. All preparations used for electron microscopy were prepared in a cold room at approximately 4°C as follows: for

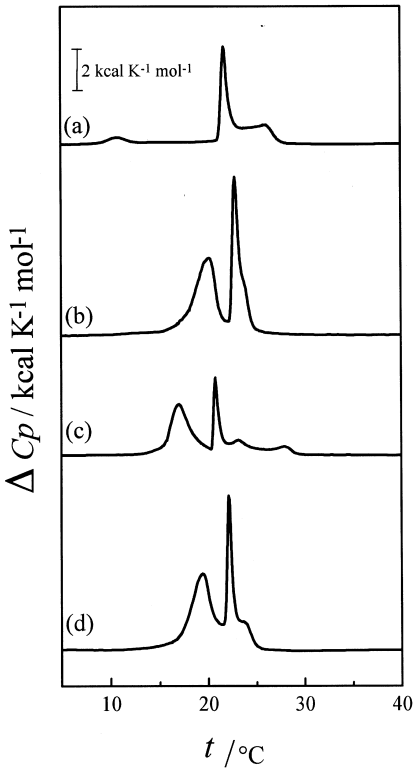

Fig. 1. Thermal behavior of DMPG in sodium phosphotungstate solutions and sodium phosphate buffers. Apparent, excess heat capacity (ΔCp) per 1 mol of lipid is plotted as a function of temperature (t). (a) DMPG vesicle prepared with 2% (w/v) sodium phosphotungstate solution ($[Na^+] = \sim 40$ mM); (b) DMPG vesicle prepared with 5% (w/v) sodium phosphotungstate solution ($[Na^+] = \sim 100$ mM), and then annealed at 5°C for 24-h periods; (c and d) DMPG vesicles prepared with sodium phosphate buffers at 15 ($[Na^+] = \sim 20$ mM) and 72 mM ($[Na^+] = \sim 100$ mM) at pH 7.0, respectively, and then annealed at 5°C for 24-h periods.

$[Na^+] \leq 100$ mM, a drop of lipid sample already stained (lipid concentration: ~ 2 mM) was placed on copper grids covered with carbon-coated collodion films, allowed to remain until becoming dry; for $[Na^+] > 100$ mM in the absence of the stainer, after a drying of lipid sample on copper grids, a drop of 2% solution of sodium phosphotungstate was added and then, the excess solution was drained. If a stain for the preparations was not sufficient, 2% solution of uranyl acetate was used. The preparations were supplied immediately to electron microscopy operated at around 20°C.

3. Results

3.1. Differential scanning calorimetry

As previously reported in our electron microscopic study [7], when Na^+ concentration is changed from 0 to 1000 mM, the number of lamellae in each DMPG vesicle in the gel phase varies from one up to approximately 30, simultaneously with a change in the mean diameter from 100 nm to 1 μm. These gel vesicles, widely differing in multiplicity and size, were incubated at 5°C for 30 days. Thermal behavior of subtransition observed during the period of annealing are roughly grouped into two types (Fig. 2A and B–E) depending on whether Na^+ concentration is above or below a boundary region of approximately 200–250 mM.

For $[Na^+] > 250$ mM, as is shown in Fig. 2A at $[Na^+] = 500$ mM, the subtransition is characterized by two peaks, denoted by T_{H1} and T_{H2}[1], at temperatures higher than the T_M transition. First, the T_{H1} peak appears as a shoulder at a high-temperature side of the T_M peak and grows at the expense of the T_M peak (b and c). However, the T_{H1} peak is replaced by the T_{H2} peak which grows at around 43°C with a further annealing (b–d). Finally, only a limiting T_{H2} peak is observed (e). The conversion to the final T_{H2} peak is completed within a relatively short period of 24 h. A repeating scan measured after a DSC of curve (e) is the same as curve (a) for the non-annealed sample (f).

Fig. 3A shows a schematic diagram of relative enthalpy (ΔH) vs. temperature (t) curves for $[Na^+] > 200$–250 mM, which were constructed on the basis of the temperatures and enthalpy changes for the T_M, T_{H1} and T_{H2} transitions shown in Fig. 2A. Therefore, enthaplies in each phase are shown to be constant although a temperature varies. By annealing, the gel phase first

[1]We don't think it appropriate to use notations T_{H1}, T_{H2}, T_{L1} and T_{L2} for each subtransition of the present system. However, to distinguish four subtransitions, these notations have been used in the present paper. The notation T_{H1} means the transition for the subgel phase H_1.

converts to a more stable phase (denoted in the diagram by H_1) characterized by the T_{H1} transition, and finally to the most stable phase (denoted by H_2) characterized by the T_{H2} transition.

For $[Na^+] < 200$ mM, as is shown in Fig. 2B–E, the subtransition is characterized by two peaks, denoted by T_{L1} and T_{L2}, which appear at temperatures lower than the T_M transition. Both peaks grow into limiting ones during the first 24-h period of annealing. When the limiting two peaks are compared, the area of T_{L2} peak at a higher temperature is larger for higher Na^+ concentrations, in contrast with the T_{L1} peak, for which the area is larger for lower Na^+ concentrations. Details in this Na^+ concentration region are as follows.

For $[Na^+] = 100$ mM (Fig. 2B), the annealing up to 24 h produces only the T_{L2} peak at approximately 20°C (b), but the T_M peak remains unchanged through a growth of the T_{L2} peak. A limiting T_{L2} peak shown in (b) is maintained over a week, after which a high-temperature subtransition peak comparable to the T_{H2} peak shown in Fig. 2A grows at the expense of both the T_{L2} and T_M peaks (c). When the annealing of a 30-day period is reached, only a limiting T_{H2} peak is observed (d). However, the limiting T_{H2} peak is splitted, also showing that the transition temperature is lower by approximately 4°C and the transition enthalpy is smaller by approximately 0.6 kcal/mol lipid, compared with the T_{H2} peak shown in (e) of Fig. 2A.

For $[Na^+] = 80$–50 mM (Fig. 2C,D), a newly produced T_{L1} peak at around 17°C grows together with the T_{L2} peak during 24-h periods of annealing [Fig. 2C(b) and D(b)]. With a further annealing, a gradual growth of the T_{H2} peak is observed for $[Na^+] = 80$ mM at the expense of the T_{L1}, T_{L2} and T_M peaks [Fig. 2C(c)]. However, a saturated T_{H2} peak is not attained, even with a 30-day period of annealing, and hence the T_{L1}, T_{L2} and T_M peaks remain in reduced sizes [Fig. 2C(d)]. In this contrast, no growth of the T_{H2} peak is observed for $[Na^+] = 50$ mM and the limiting T_{L1}

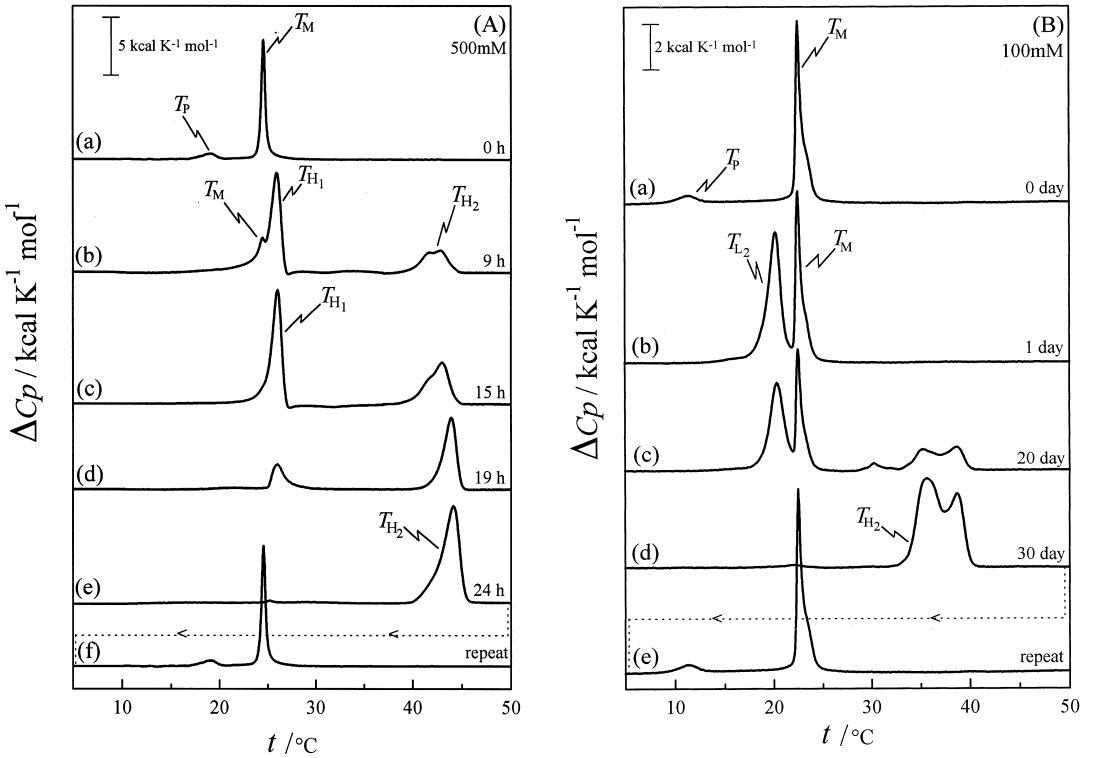

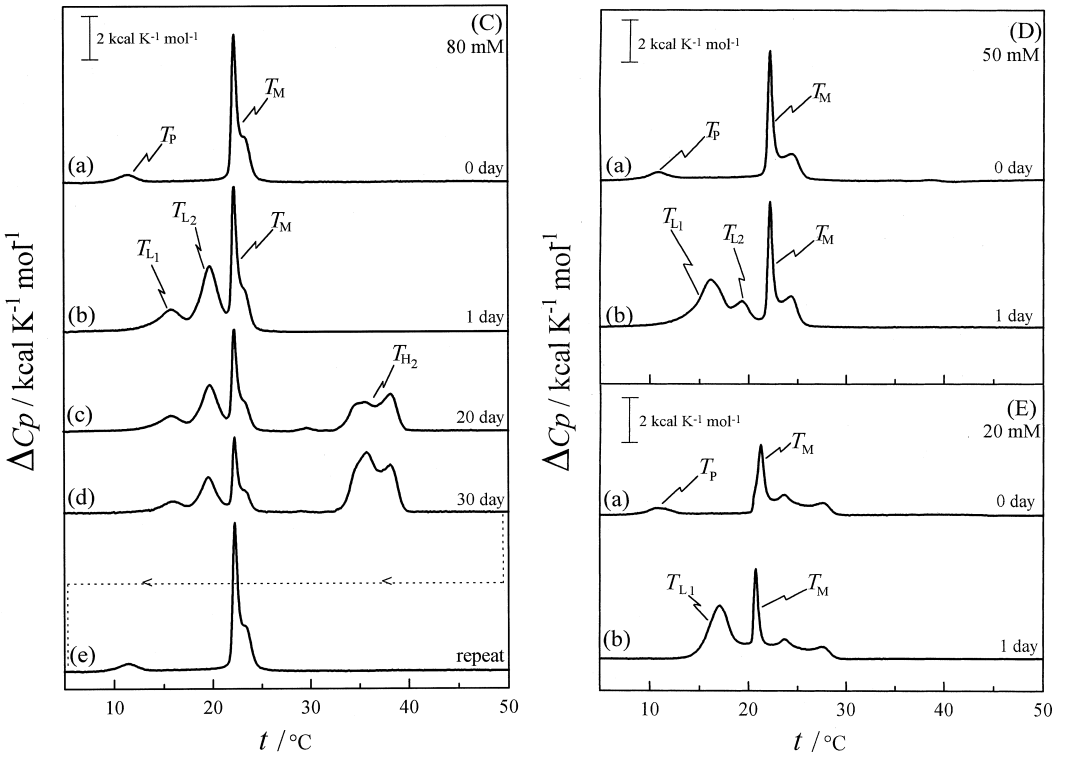

Fig. 2. Typical thermal behavior of DMPG in NaCl solutions at different concentrations observed during periods of annealing (at 5°C) up to 30 days. Apparent, excess heat capacity (ΔCp) per 1 mol of lipid is plotted as a function of temperature (t). [Na^+]: (A) 500, (B) 100, (C) 80, (D) 50, and (E) 20 mM. Annealing periods: for (A): (a) 0, (b) 9, (c) 15, (d) 19, (e) 24 h; for (B and C): (a) 0, (b) 1, (c) 20, (d) 30 days; for (D and E): (a) 0, (b) 1 day. A final DSC curve in each figure shows a repeating scan measured after a DSC for a sample annealed for 30 days.

and T_{L2} peaks remain unaltered over a period of 30 days.

For $[Na^+] = 20$ mM (Fig. 2E), the annealing produces almost only the T_{L1} peak (b). A limiting T_{L1} peak is held constant over a 30-day period, and hence the T_{H2} peak is not detected, similarly to $[Na^+] = 50$ mM. In addition, for $[Na^+] = 0$ mM, thus, in the absence of NaCl, any appreciable change is not observed up to 30 days of annealing.

Fig. 3B shows a schematic diagram of ΔH vs. temperature curves for 20 mM $\leq [Na^+] < 200$ mM, which summarizes all the phase behavior shown in Fig. 2B–E. The transition enthalpies of T_{L1} and T_{L2} shown in the diagram were estimated by a method described in the text. The conversion of the gel to subgel phases at the primary stage of annealing up to 24 h is as follows; for 100 mM $\leq [Na^+] < 200$ mM, all of the gel phase converts to a more stable subgel phase (denoted in the diagram by L_2) characterized by the T_{L2} transition; for 20 mM $< [Na^+] < 100$ mM, some of the gel phase converts to the L_2 phase and the remainder to a less stable subgel phase (denoted by L_1) characterized by the T_{L1} transition; and for $[Na^+] = 20$ mM, only conversion into the L_1 phase takes place.

On the other hand, for the boundary region of $[Na^+] = 200$–250 mM, the phase behavior is complicated and the conversion to the T_{H2} peak proceeds with the appearance of T_{L2} and T_{H1} peaks during a10-day period of annealing.

To quantitatively elucidate the conversion of the gel phase to either L_1 or L_2 phases for $[Na^+] < 200$ mM, the fraction F_{L2} occupied by the L_2 phase was estimated from the enthalpy

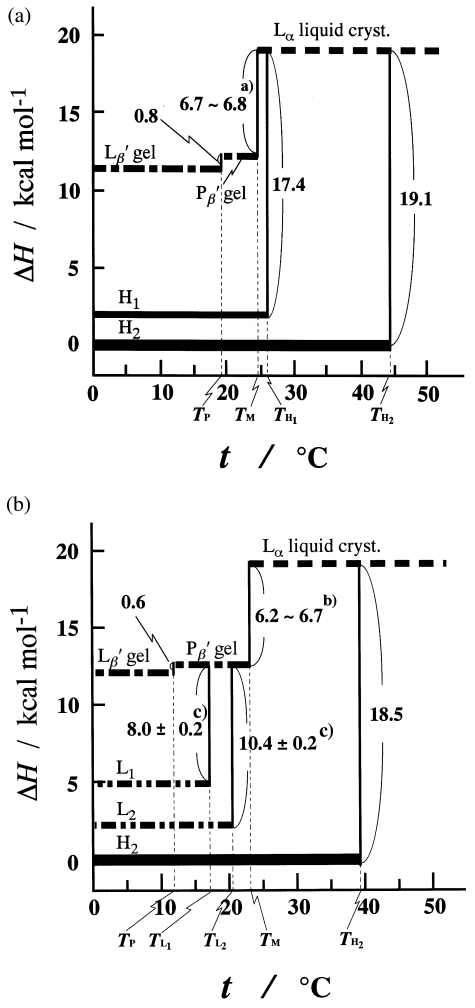

Fig. 3. Schematic diagrams of relative enthalpy (ΔH) vs. temperature (t) at Na^+ concentrations (a) above and (b) below 200–250 mM for the gel, liquid crystal and subgel phases (H_1, H_2, L_1 and L_2) of DMPG. a) T_M transition enthalpies change from 6.7 to 6.8 kcal/mol lipid with an increase in Na^+ concentration from 200 to 1000 mM [7]. b) T_M transition enthalpies change from 6.2 to 6.7 kcal/mol lipid with an increase in Na^+ concentration up to 200 mM [7]. c) T_{L1}, T_{L2} and T_{H1} transition enthalpies were estimated from a deconvolution analysis with the average standard deviation of 0.2 kcal/K·mol.

changes of the limiting T_{L2} peaks obtained by a deconvolution analysis and the remainder, $1 - F_{L2}$, was taken as the fraction F_{L1} occupied by the L_1 phase. All DSC curves (b) in Fig. 2B–E were deconvoluted by a computer program (ORIGIN, Microcal Software Inc.) according to a multiple Gaussian curve analysis. Results of the deconvolution analyses are compared in Fig. 4. Focusing on the subtransition peaks, a single component of deconvoluted curve T_{L2} is observed for $[Na^+] = 100$ mM (Fig. 4d), in contrast with two components of deconvoluted curves T_{L1} and T_{L2} for $[Na^+] < 100$ mM (Fig. 4a–c). Since the enthalpy change ($= 10.4 \pm 0.2$ kcal/mol lipid) of the single deconvoluted curve T_{L2} ($F_{L2} = 1$) corresponds to a molar transition enthalpy for the T_{L2} transition, the fraction F_{L2} was estimated from $F_{L2} = \Delta H_{L2}/10.4$, where ΔH_{L2} is the enthalpy change of individual deconvoluted curves T_{L2} shown in Fig. 4a–c. The resulting values of F_{L2} are plotted against Na^+ concentration in Fig. 5, together with the F_{L1} ($= 1 - F_{L2}$). The average value of molar transition enthalpies for the T_{L1} transition was estimated from $\Delta H_{L1}/F_{L1}$, where ΔH_{L1} is the enthalpy change of individual deconvoluted curves T_{L1} shown in Fig. 4a–c. The resulting molar transition enthalpy of T_{L1} (8.0 ± 0.2 kcal/mol lipid) is shown in Fig. 3B, together with that of T_{L2}. The point to notice in Fig. 5 is that the F_{L2} increases with an increase in Na^+ concentration, contrary to the behavior of the F_{L1}.

3.2. Electron microscopy

The structures of L_1, L_2 and H_2 phases were investigated by electron microscopy, in comparison with our previous study with $[Na^+] = 1000$ mM [8]. For micrographs of gel (a), L_2 (c) and H_2 phases (d) shown in Fig. 6, samples at $[Na^+] = 100$ mM were used as (a), (b) and (d) of Fig. 2B, respectively. For a micrograph of L_1 phase (b), a sample at $[Na^+] = 20$ mM characterized by curve (b) of Fig. 2E was used, although it contains the L_2 phase by approximately 8% in fraction, as shown in Fig. 5. For the L_2 phase shown in Fig. 6c, several lamellae are observed to be regularly and closely stacked in a two-dimensional belt-like structure, which is comparable to a structure of DPPG subgel phase previously reported by other workers [15,16]. The L_1 phase shown in Fig. 6b is also the belt-like structure, but loose and irregular stacks of lamellae are observed. For the H_2 phase in Fig. 6d, 8–10 lamellae are wrapped in a

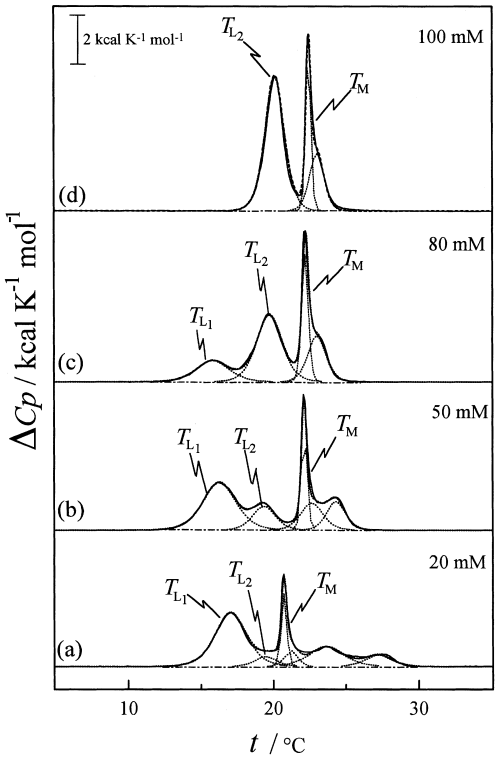

Fig. 4. Deconvolution analyses of DSC curves for the T_{L1} and T_{L2} subtransitions of DMPG at Na^+ concentrations of (a) 20, (b) 50, (c) 80 and (d) 100 mM. The deconvolutions were performed on the basis of a computer program ORIGIN for Gaussian curve analysis attached to a Microcal calorimeter [25]. The T_M transition peaks were also deconvoluted because of overlapping the subtransition peaks. In each figure, deconvoluted T_{L1} and T_{L2} curves, deconvoluted T_M curves and a sum of these deconvoluted curves (i.e. a theoretical curve) are shown by dotted lines, compared with the experimental DSC curve shown by a solid line. The theoretical curve was well fitted to the experimental curve with the average standard deviation of 0.2 kcal/K per mol. The apparent, excess heat capacity (ΔCp) per 1 mol of lipid is plotted against temperature (t).

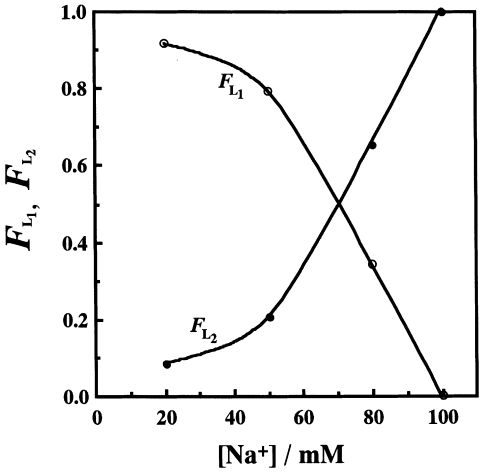

Fig. 5. Variations of fractions occupied by the L_1 and L_2 subgel phases with Na^+ concentration. F_{L1} and F_{L2} are fractions occupied by the L_1 and L_2 phases, respectively.

cylinder and a group of the H_2 phase is shown in Fig. 6e. Such a cylindrical superstructure has been already reported for $[Na^+] = 1000$ mM in our previous paper [8].

4. Discussion

Fig. 3A,B indicate that the H_2 phase is thermodynamically stable, but other phases such as gel, L_1, L_2 and H_1 are metastable. Furthermore, it is shown that there are two pathways for the conversion of DMPG gel vesicles to a final destination of the most stable H_2 phase by annealing. The two pathways differ in an intermediate phase which appears on the way to attainment of the H_2 phase. Thus, the pathway A for $[Na^+] > 250$ mM is by way of the H_1 phase and the pathway B for $[Na^+] < 200$ mM is by way of the L_2 phase. As previously reported by us [7], the non-specific shielding effect of Na cation, due to a diffuse double layer, on negatively charged DMPG gel vesicle reaches a saturation at approximately $[Na^+] = 200$ mM. Accordingly, the selection of either pathways A (H_1 phase) or B (L_2 phase) depends on whether Na^+ concentration is above or below the saturation point. As is obvious from Fig. 3, the intermediate H_1 and L_2 phases differ in the transition mode to the liquid crystal phase. However, belt-like lamellar stacks similar to the L_2 phase shown in Fig. 6c have already been observed for the H_1 phase [8]. Considering such a structural resemblance between both intermediate phases, it is presumed that the conversion process is essentially the same for pathways A and B. Thus, although the gel phase results from the isomerization of hydrocarbon chains from

gauche to *trans* by a cooling to temperatures below the T_M transition, the hydrocarbon chains of the gel phase are not so close together as expected for their *trans* form. So, a narrowing of the chain–chain distance gradually proceeds at the primary stage of annealing. However, for DMPG having negatively charged head group, it is required to reduce a repulsion space between adjacent head groups. For this, a specific shielding effect of Na cation would be required in such a way that external bulk Na cations condense on the surface of the vesicle. Such an action of the cations leads to a decrease in the surface curvature of the outermost lamellar in each vesicle [7], so that the lamellar separation from the vesicle shown by Fig. 6f occurs. All lamellae surrounding the vesicle separate successively, as shown by Fig. 6g, and exist in a belt-like lamellar stack, more or less, in a helical structure, which corresponds to the intermediate L_2 and H_1 phases. At the secondary stage of annealing, the lamellar stack enhances its helical structure, and finally reaches a limiting, maximum helix corresponding to the H_2 phase of cylindrical superstructure shown in Fig. 6d.

As shown in Fig. 3B, although there are structural differences in the multiplicity and size among DMPG vesicles for $[Na^+] < 200$ mM, their destinations at the primary stage of annealing are limited to two subgel phases of L_1 and L_2. This indicates that two types of lipid packings are allowed for the metastable subgel phase of DMPG in this Na^+ concentration. In this connection, it is noticeable that the transition temperatures of both subgel phases are almost fixed at T_{L1} and T_{L2}, respectively, regardless of Na^+ concentration (Fig. 4), although their fractions depend on Na^+ concentration (Fig. 5). Such Na^+ concentration-independent-subtransition temperatures suggest that the L_1 and L_2 phases at each Na^+ concentration incorporate interlamellar Na cation in constant amounts, respectively, which are required to realize closer chain packings for both phases, compared with the gel phase. However, irregularly and rather loosely stacked lamellae of the L_1 phase (Fig. 6b) indicate a less amount of interlamellar Na cations for this phase than for the L_2 phase of closely stacked lamellae (Fig. 6c). Because of such a structural irregularity, the L_1 phase is unable to convert into a more ordered structure of the H_2 phase at the secondary stage of annealing (Fig. 2E). In this contrast, the L_2 phase completely converts to the H_2 phase (Fig. 2B). Furthermore, it is suggested that the incorporation of interlamellar Na cation in a desired amount, especially for the L_2 phase, causes an imbalance in Na^+ concentration between interlamellar and external bulk regions. Therefore, to minimize the imbalance, as is shown in Fig. 5, the fraction of the L_2 phase rich in interlamellar Na cation is diminished by a decrease in Na^+ concentration, contrary to the fraction of the L_1 phase.

So far many studies of phase behavior of PGs

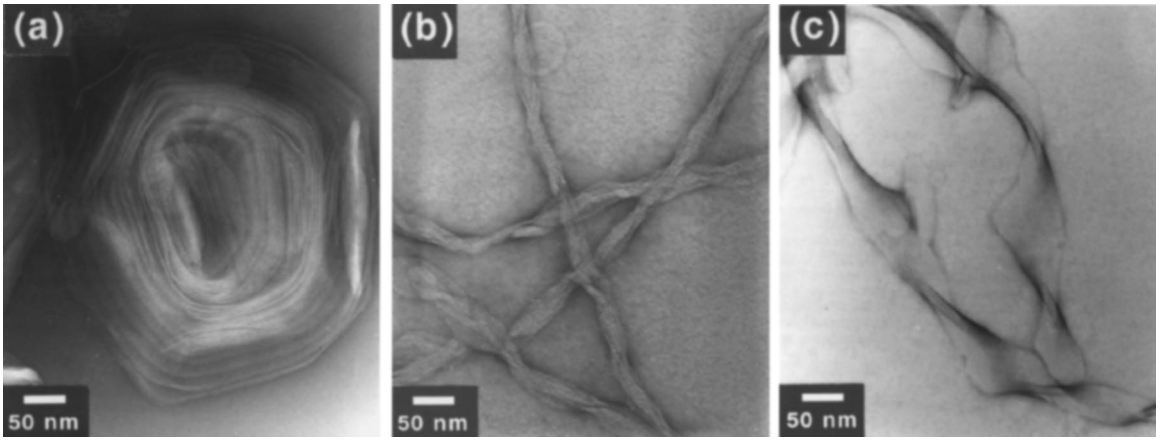

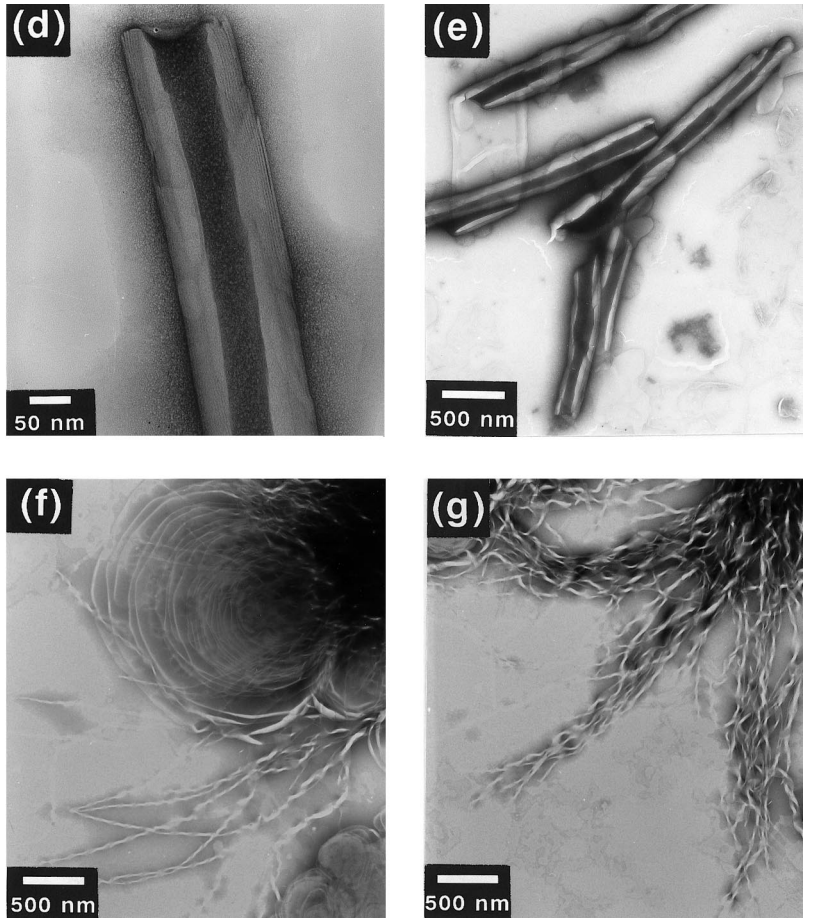

Fig. 6. Electron micrographs of DMPG assemblies: (a) a multilamellar vesicle in the gel phase prepared at $[Na^+] = 100$ mM; (b) loosely stacked lamellae in a belt-like structure (L_1 phase) observed after annealing (at 5°C for 1 day) for a vesicle prepared at $[Na^+] = 20$ mM; (c) closely stacked lamellae in a belt-like structure (L_2 phase) observed after annealing (at 5°C for 1 day) for the vesicle (a); (d) a superstructure composed of lamellae wrapped in a cylinder (H_2 phase) observed after annealing (at 5°C for 30 days) for the vesicle (a); (e) a group of cylindrical superstructures; (f) lamellar separations observed at the beginning of annealing; and (g) a great number of lamellae separated from the vesicle

have been performed with a variety of buffers, simultaneously in the presence or absence of various salts at different concentrations [1–6,15–19]. However, for comparisons of these past studies, it is required to pay particular attention to coexisting cations, by which a lateral packing of PG molecules is greatly affected. In this connection, to investigate the effect on the subgel phase by sodium cation contained as a component of buffer, DMPG vesicles prepared with sodium phosphate buffers (at pH 7.0) at different concentrations of 15 and 72 mM ($[Na^+]$: ~ 20 and ~ 100 mM) were annealed at 5°C over a period of 24 h and compared with the results in NaCl solutions shown in Fig. 2. Thermal behavior in the buffer solutions shown in c and d of Fig. 1 is almost comparable to that shown in B(b) and E(b) of Fig. 2 at the corresponding Na^+ concentrations, respectively, indicating the same function for both sodium cations derived from phosphate buffer and NaCl.

According to the above-discussed result, to compare with DPPG subgel phase in 50 mM sodium phosphate buffer ([Na]: ~ 70 mM) previ-

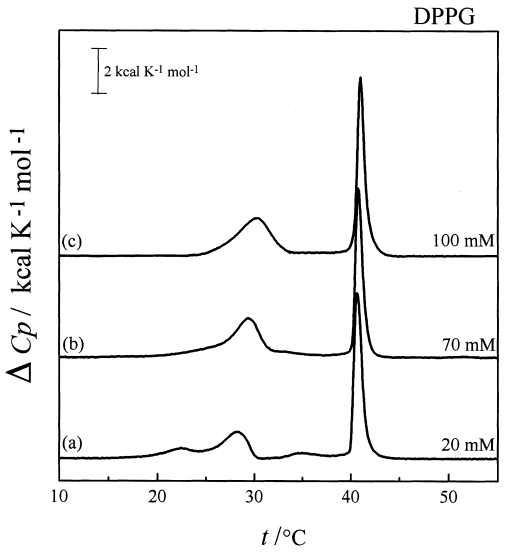

Fig. 7. Thermal behavior observed after annealing (at 5°C for at least 30 days) for DPPG vesicles prepared with NaCl solutions at concentrations of (a) 40, (b) 70 and (c) 100 mM. Apparent, excess heat capacity (ΔCp) is plotted as a function of temperature (t).

ously reported by Wilkinson [15] and Blaurock [16], DPPG vesicles prepared with 40, 70 and 100 mM NaCl aqueous solutions were annealed over a period of at least 30 days. As shown in Fig. 7, the resulting subtransition peaks of DPPG show Na^+ concentration-dependent-behavior similar to DMPG subtransition peaks shown in Fig. 4. Thus, the double-peaked subtransition shown in a and b of Fig. 7 indicates a two-subgel phase system for DPPG, although it has been treated as a single subgel phase by previous workers [15,16]. The total enthalpy changes of the subtransitions characterized by a single or double peaks shown in Fig. 7 are 6.3, 7.4 and 8.4 kcal/mol lipid for a, b and c, respectively. The molar subtransition enthalpies (ΔH_{L1} and ΔH_{L2}) for the L_1 and L_2 phases of DPPG were estimated from the deconvolution analysis used for DMPG. The resulting values are 4.6 ± 0.2 and 8.4 ± 0.2 kcal/mol lipid for the ΔH_{L1} and ΔH_{L2}, respectively, and fairly smaller than the corresponding subtransition enthalpies of DMPG (thus, 8.0 and 10.4 ± 0.2 kcal/mol lipid). The smaller subtransition enthalpy for DPPG is the opposite chain length-dependence to that of the T_M transition enthalpy which is larger for longer chains, thus, 6.4 and 8.5 kcal/mol lipid for DMPG and DPPG, respectively.

In a series of studies, the Nagle group [22–24] has revealed a large contribution of the change in the van der Waals interaction energy of the hydrocarbon chains to the transition enthalpies in lipid–water systems. However, data of X-ray diffraction and dilatometry are necessary for estimations of the van der Waals interaction energy. So, by using the data for DPPG in 50 mM sodium phosphate buffer obtained by Wilkinson et al. [5,15], although their data for the subgel phase are ones for a two phase system of L_1 plus L_2, the difference in the van der Waals interaction energy between the $L_{\beta'}$ gel and subgel phases for DPPG, ΔU_{vdw}, was calculated from a formula previously developed by Nagle et al. [22,23];

$$\Delta U_{vdw} = -(2.3 \text{ kcal}) \left[(r_o / r_{L\beta' gel})^5 - (r_o / r_{subgel})^5 \right] \text{kcal/mol CH}_2, \quad (1)$$

where r_o is the nearest neighbor separation between hydrocarbon chains at 0 K and $r_{L\beta' gel}$ and r_{subgel} are the chain separations for the $L_{\beta'}$ gel and subgel phases at the same temperature, respectively. The chain separation, $r_{L\beta' gel}$ for the $L_{\beta'}$ gel phase was obtained from the volume per CH_2 group, $V_{CH2} = (1.27 \text{ Å})(\sqrt{3}/2)\ r^2 \text{Å}^3$, based upon approximate hexagonal packing of the hydrocarbon chains. In the same manner, r_{subgel} for the subgel phase was estimated although its X-ray wide angle reflection is further from hexagonal than the $L_{\beta'}$ gel phase [15]. First, V_{CH2} for the $L_{\beta'}$ gel phase of DPPG as a function of temperature was calculated from the X-ray spacing ($d = 4.25$ Å at 20°C) and the thermal expansion coefficient ($\alpha = 105 \times 10^{-5}$ ml/g·deg $= 1.30$ Å^3/molecule·deg) for this phase [5,15] as follows; the V_{CH2} for the $L_{\beta'}$ gel phase at 20°C was calculated to be $1.27 \text{ Å} \times (\sqrt{3}/2) \times (4.25 \text{ Å})^2 = 26.5_1$ Å^3, and then extrapolated back to 0°C and up to the T_p temperature using the coefficient of thermal expan-

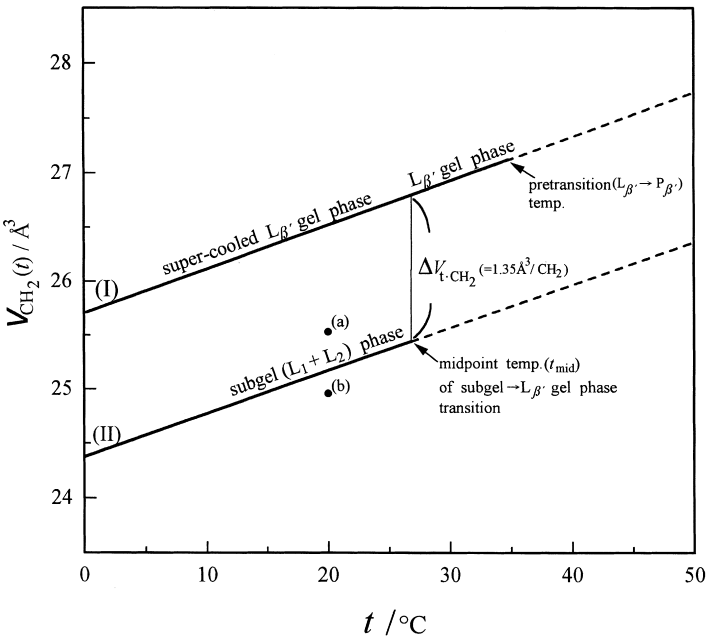

Fig. 8. Volume per CH_2 group of the hydrocarbon chains (V_{CH2}) as a function of temperature (t) for (I) the $L_{\beta'}$ gel and (II) subgel (L_1 plus L_2) phases of DPPG estimated from data of X-ray diffraction and dilatometry by Wilkinson et al. [5,15]. (a and b): V_{CH2} at 20°C for the L_1 and L_2 subgel phases of DPPG calculated from the T_{L1} and T_{L2} subtransition enthalpies, respectively.

sion per CH_2 group, $\alpha_{CH2} = (1/32) \times 1.30$ Å^3/molecule·deg = 0.0406 Å^3/CH_2·deg. The resulting $V_{CH2} = 25.70 + 0.0406\ t$ for the $L_{\beta'}$ gel phase of DPPG are shown in curve I of Fig. 8.

On the other hand, V_{CH2} for the subgel phase as a function of temperature was calculated from the X-ray spacing ($d = 4.11$ Å at 10°C) for this phase and the volume change (ΔVt = 0.035 ml/g = 43.3 Å^3/molecule) associated with the subtransition [15] as follows; the V_{CH2} for the subgel phase at 27°C (the midpoint temperature of the subtransition), 25.4 Å^3, was calculated by subtracting the volume change per CH_2 group at the subtransition, $\Delta V t_{CH2} = (1/32) \times 43.3$ Å^3/molecule = 1.35 Å^3/CH_2, from the V_{CH2} for the $L_{\beta'}$ gel phase at the same temperature obtained from curve I, 26.8 Å^3/CH_2, and then used to calculate the coefficient of thermal expansion per CH_2 group for the subgel phase, $\alpha_{CH2} = 0.0396$ Å^3/CH_2·deg, with the aid of the V_{CH2} at 10°C, 1.27 Å $\times (\sqrt{3}/2) \times (4.11$ Å$)^2 = 24.8$ Å^3. The resulting $V_{CH2} = 24.38 + 0.0396\ t$ for the subgel phase is shown in curve II of Fig. 8. As shown in Fig. 8, the α_{CH2} is almost the same for curves I and II, indicating that the difference in the V_{CH2} between the $L_{\beta'}$ gel and subgel phases is nearly the same at any temperature below the subtransition. Reflecting this phenomenon, values of ΔU_{vdw} [$= U_{vdw}(L_{\beta'}gel) - U_{vdw}$(subgel)] calculated from Eq. (1) reveal only small temperature dependence such as 6.8, 6.5 and 6.3 kcal/mol lipid at 10, 20 and 27°C, respectively. Furthermore, ΔU_{vdw} calculated at the neighborhood of the subtransition temperature are found to be close to the total transition enthalpy (6.3 kcal/mol) for the double peaked subtransition (Fig. 7a) obtained by us. This result indicates that the origin of the subtransition enthalpy is almost a change in the van der Waals interaction energy of hydrocarbon chains caused by a shorter chain separation for the subgel phase than for the $L_{\beta'}$ gel phase.

Based upon the above-discussed result that ΔU_{vdw} at the neighborhood of the subtransition temperature is nearly equal to the calorimetric

subtransition enthalpy, the molar subtransition enthalpies of T_{L1} and T_{L2} (4.6 and 8.4 kcal/mol) for DPPG obtained by us were used to calculate the r_{subgel} at 20°C for each of the L_1 and L_2 subgel phases from Eq. (1) using the $r_{L\beta'gel}$ (= 4.91 Å, at 20°C) obtained from curve I shown in Fig. 8. In the calculation for the r_{subgel} for the L_2 phase, the subtransition enthalpy into the $L_{\beta'}$ gel phase, 7.6 [= 8.4 − 0.8 (T_p transition enthalpy)] kcal/mol, was used, by considering no pretransition in curve c of Fig. 7. The resulting values of r_{subgel} at 20°C are 4.8_2 and 4.7_6 Å for the L_1 and L_2 phases, respectively. For a comparison with V_{CH2} for the (L_1 plus L_2) phases shown in curve II of Fig. 8, the V_{CH2} for each subgel phase was also estimated at 20°C and are shown in the same figure.

There is some uncertainty in the above calculations because the hexagonal array is substituted for the chain packing of the subgel phases of DPPG. However, it seems to be proved that the difference in the enthalpy between the L_1 and L_2 phases of DPPG relative to the $L_{\beta'}$ gel phase comes from the difference in the van der Waals interaction energy caused by the difference in the chain–chain separation between both subgel phases. The same result holds also for the L_1 and L_2 phases of DMPG, thus, indicating that the enthalpy difference, 2.4 kcal/mol, shown in Fig. 3B is caused by a closer chain packing for the latter than for the former. Presumably, a larger amount of interlamellar Na cations for the L_2 phase (discussed above) causes a greater shielding effect on the head groups, resulting in a shorter chain separation for this phase, compared with the L_1 phase.

Finally, focusing on the present result that the van der Waals interaction energy of the hydrocarbon chains is a determinant for the enthalpy of lipid assemblies in a *trans* form, a little or almost no chain-length dependence could be suggested for the chain separation of the subgel phase, in contrast to the chain separation of the gel phase which is longer for shorter chains [22]. As a result, the ΔU_{vdw} between the gel and subgel phases becomes larger for shorter chains, and this causes the larger subtransition enthalpy for DMPG than for DPPG observed in the present study.

Acknowledgements

We thank Prof. J.F. Nagle (Carnegie-Mellon University) for his useful comments and advises. This work was supported by the Grant-in-Aid for Scientific Research Nos. 08640748 (1996) and 09640702 (1997–1998) from the Ministry of Education, Science and Culture in Japan, and also by the Special Grant for Cooperative Research administered by Japan Private School Promotion Foundation (1996–2001).

References

[1] A. Watts, K. Harlos, W. Maschke, D. Marsh, Biochim. Biophys. Acta 510 (1978) 63–74.
[2] A. Watts, K. Harlos, D. Marsh, Biochim. Biophys. Acta 645 (1981) 91–96.
[3] J.L. Ranck, J.F. Tocanne, FEBS Lett. 143 (1982) 171–174.
[4] J.L. Ranck, J.F. Tocanne, FEBS Lett. 143 (1982) 175–178.
[5] D.A. Wilkinson, D.A. Tirrell, A.B. Turek, T.J. McIntosh, Biochim. Biophys. Acta 905 (1987) 447–453.
[6] H. Takahashi, S. Matuoka, S. Kato, K. Ohki, I. Hatta, Biochim. Biophys. Acta 1110 (1992) 29–36.
[7] M. Kodama, T. Miyata, Thermochim. Acta 267 (1995) 365–372.
[8] M. Kodama, T. Miyata, T. Yokoyama, Biochim. Biophys. Acta 1168 (1993) 243–248.
[9] A.J. Verkleij, B. De Kruyff, P.H.J. Th. Ververgaert, J.F. Tocanne, L.L.M. Van Deenen, Biochim. Biophys. Acta 339 (1974) 432–437.
[10] P.H.J. Th. Ververgaert, B. De Kruyff, A.J. Verkleij, J.F. Tocanne, L.L.M. Van Deenen, Chem. Phys. Lipids 14 (1975) 97–101.
[11] P.W.M. Van Dijck, P.H.J. Th. Ververgaert, A.J. Verkleij, L.L.M. Van Deenen, J. De Gier, Biochim. Biophys. Acta 406 (1975) 465–478.
[12] K. Jacobson, D. Papahadjopoulos, Biochemistry 14 (1975) 152–161.
[13] P.W.M. Van Dijck, B. De Kruijff, A.J. Verkleij, L.L.M. Van Deenen, J. De Gier, Biochim. Biophys. Acta 512 (1978) 84–96.
[14] J.M. Boggs, G. Rangaraj, Biochemistry 22 (1983) 5425–5435.
[15] D.A. Wilkinson, T.J. McIntosh, Biochemistry 25 (1986) 295–298.

[16] A.E. Blaurock, T.J. McIntosh, Biochemistry 25 (1986) 299–305.
[17] K.K. Eklund, I.S. Salonen, P.K.J. Kinnunen, Chem. Phys. Lipids 50 (1989) 71–78.
[18] I.S. Salonen, K.K. Eklund, J.A. Virtanen, P.K.J. Kinnunen, Biochim. Biophys. Acta 982 (1989) 205–215.
[19] R.M. Epand, B. Gabel, R.F. Epand, A. Sen, S.W. Hui, A. Muga, W.K. Surewicz, Biophys. J. 63 (1992) 327–332.
[20] A.D. Bangham, M.W. Hill, N.G. Miller, Methods Membr. Biol. 1 (1974) 168.
[21] G.V. Marinetti, J. Lipid Res. 3 (1962) 1–20.
[22] J.F. Nagle, D.A. Wilkinson, Biophys. J. 23 (1978) 159–175.
[23] D.A. Wilkinson, J.F. Nagle, Biochemistry 20 (1981) 187–192.
[24] D.A. Wilkinson, J.F. Nagle, Biochemistry 23 (1984) 1538–1541.
[25] H. Aoki, M. Kodama, Thermochim. Acta 308 (1998) 77–83.